Dual Electrical Behavior of Multivalent Metal Cation-Based Oxide and Its Application to Thin-Film Transistors with High Mobility and Excellent Photobias Stability

Myeong Gu Yun, Cheol Hyoun Ahn, Sung Woon Cho, So Hee Kim, Ye Kyun Kim, and Hyung Koun Cho*

School of Advanced Materials Science and Engineering, Sungkyunkwan University, Suwon, 440-746, Korea

Ⓢ *Supporting Information*

ABSTRACT: The effect of multivalent metal cations, including vanadium(V) and tin (Sn), on the electrical properties of vanadium-doped zinc tin oxide (VZTO) was investigated in the context of the fabrication of thin-film transistors (TFTs) using a single VZTO film and VZTO/ZTO bilayer as channel layers. The single VZTO TFT did not show any response to the gate voltage (insulator-like behavior). On the other hand, the VZTO/ZTO bilayer TFT exhibited a typical TFT transfer characteristic (semiconducting behavior). X-ray photoelectron spectroscopy revealed that, in contrast to what is commonly true in many oxides, oxygen vacancies (V_O) in VZTO did not provide a dominant contribution to the total carrier concentration, because the V_O peak area in the single VZTO film was 5.4% and reduced to 4.5% in VZTO/ZTO bilayer. Instead, Sn $3d_{5/2}$ and V $2p_{3/2}$ spectra suggest that the significant reduction in Sn and V ions is strongly related to the insulator-like behavior of the VZTO film. In negative-bias illumination tests and illumination tests with various photon energies, the VZTO/ZTO bilayer TFT had much better stability than the ZTO TFT. This result is attributed to the reduction of donor-like states (V_O) that can be positively ionized by blue and green illumination.

KEYWORDS: *multivalent metal cation, dual electrical property, oxide semiconductor, thin film transistor, stability*
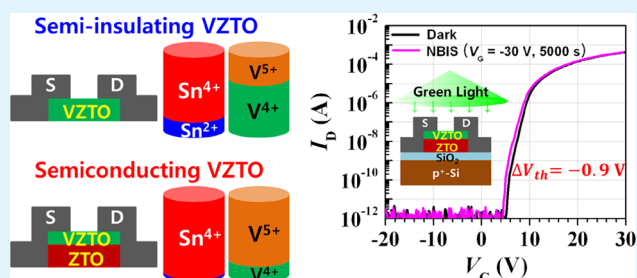
1. INTRODUCTION

Amorphous oxide semiconductors (AOSs), including ZnSnO (ZTO),[1] InZnO,[2] InGaO,[3] and InGaZnO,[4] have garnered much attention as channel materials for thin-film transistors (TFTs), because of their use in displays with high resolution, fast response time, large area, transparency, and/or flexibility. This practical worth of AOSs originates from the fact that even if an oxide semiconductor is deposited at a low process temperature, in order to be a thin film of amorphous phase with good uniformity, the mobility is still high (usually >10 cm² V⁻¹ s⁻¹), unlike the previous channel material (amorphous Si).[4] Furthermore, AOSs have the benefit of being transparent. Among various AOS TFTs, current commercialized AOS TFTs adopt InGaZnO as the channel material. There are two reasons for this. First, among AOSs, IGZO is the most studied and the most well understood. Second, the IGZO TFT has sufficient reliability for mass production. In the meantime, ZTO TFTs have also drawn considerable attention, because of their comparable or better TFT performance and much lower raw material costs when compared with InGaZnO TFTs. However, unlike InGaZnO TFTs, the inferior stability of ZTO TFTs under a variety of stresses such as bias, temperature, illumination, and their combinations still remains a major obstacle for commercialization. In particular, the negative-bias illumination stress (NBIS) is a significant issue that must be

overcome for applications in active matrix liquid crystal displays (AMLCDs) or transparent active matrix organic light-emitting diode (AMOLED) displays, since, for most operation times, the TFTs are stressed by a negative gate bias and are exposed to visible light emitted by the underlying backlight unit in AMLCDs or ambient light in transparent AMOLED displays.[5,6]

The stability can be improved by suppressing instability events of the channel-layer that include: (i) trapping of carriers or accumulation of charged defects at the gate insulator/semiconductor interface;[7,8] (ii) defect generation in the bulk semiconductor;[9−11] and (iii) interaction with ambient gases at the back surface of the channel layer.[12,13] Therefore, researchers have tried many methods such as plasma or ozone treatment of the gate insulator/semiconductor interface or the back surface,[14−16] passivation of the back surface,[12,13] insertion of an ultrathin positive charge barrier,[17] channel-thickness control,[15,17,18] multistacking of the channel layer,[19−22] and additional element incorporation (called "doping" here).[23−25] The main goal of these methods is the control of defects such as oxygen vacancies, impurities, and back-surface-adsorbed chemicals. Among defects that possibly exist in AOSs, oxygen

vacancies (V_O) have been recognized as the main cause of the NBIS instability.[8−11,26−28] V_O can be ionized to V_O^{2+} and can donate two carrier electrons to the channel during light illumination. This increased carrier concentration results in a negative shift of the threshold voltage (V_{th}). Moreover, the doubly ionized oxygen vacancies (V_O^{2+}) can move to the gate insulator/semiconductor interface when exposed to a negative bias and can be accumulated or trapped at the interface. These V_O^{2+} at the interface cause downward band bending near the interface and, consequently, lead to a negative shift in V_{th}. Thus, some metal cations, such as Hf,[23] Ga,[24] and Zr,[25] have been considered as additional elements to suppress the formation of V_O and to some extent, relatively improved stability was reported. However, the suppression of V_O also led to the severe degradation of mobility and on-current, because the V_O also acts as a carrier generator, and the mobility of an AOS is generally proportional to the carrier concentration.[29] Therefore, bilayer structures such as HIZO (0.15 mol % HfO_2)/HIZO (0.23 mol % HfO_2),[19] HIZO/IZO,[20] and ZTO/IZO[22] have been designed as a trade-off strategy to catch both high mobility and high stability and showed relatively good performance and stability.

Among unexploited doping elements in ZTO material system, vanadium (V) is well worth considering as a V_O suppressor in ZTO material system, based on the previous results of first-principle calculation in which the Gibbs free energy for the formation of V_O in VO_2 was 4.83 eV and was <3.13 eV in ZnO or <3.49 eV in SnO_2.[30,31] Also, the bond-dissociation energy that is required to dissociate the bond between vanadium and oxygen is larger than the cases of Zn or Sn (V−O: 637 kJ/mol, Zn−O: ≤ 250 kJ/mol, Sn−O: 528 kJ/mol);[32] this fact raises our expectation about elemental vanadium (V) as a possible V_O suppressor. In addition, like the Sn atom, which has two ionic forms (Sn^{4+} and Sn^{2+}), V atoms are multivalent and can be V^{5+}, V^{4+}, V^{3+}, and V^{2+}. In fact, besides actinides and lanthanides, there are many multivalent metal elements:[33]

Ti (+2, +3, +4)
V (+2, +3, +4, +5)
Cr (+2, +3, +6)
Mn (+2, +3, +4, +6, +7)
Fe (+2, +3, +6)
Co (+2, +3)
Cu (+1, +2)
Nb (+3, +5)
Mo (+2, +3, +4, +5, +6)
Ru (+3, +4, +5, +6, +8)
Pd (+2, +4)
Sn (+2, +4)
Re (+2, +4, +5, +6, +7)
Os (+2, +3, +4, +6, +8)
Ir (+2, +3, +4, +6)
Pt (+2, +4, +6)
Au (+1, +3)
Hg (+1, +2)
Tl (+1, +3)
Pb (+2, +4)

(the numbers in the parentheses indicate possible oxidation states). However, although their different charge states in an oxide material may affect overall electrical properties, so far, most of the previous reports have explained the origin of

electrical conductivity of an oxide semiconductor as point defects, such as V_O, interstitials (Zn_i, H_i, etc.),[27,34−37] or composition ratio of metal cations, in particular, the indium ratio in InZnO,[28] InGaZnO,[29] HfInZnO,[38] etc. In fact, there are few studies about the effect of the charge states of multivalent metal cations (including V and Sn) on the electrical properties of the metal oxide semiconductor.

In this study, we first introduce the multivalent V cation as a dopant into the ZTO channel layer and demonstrate that a ZTO-based bilayer TFT with high mobility and high stability can be fabricated by adopting a V-doped ZTO (VZTO)/ZTO stack as a channel structure. We also report a surprising result that the VZTO films have a dual electrical property, depending on channel structure: (i) a single VZTO film behaves like a semi-insulator, and (ii) the top VZTO film in the VZTO/ZTO stack shows semiconducting properties appropriate to a channel layer of TFT. X-ray photoelectron spectroscopy (XPS) results revealed that the multivalent cations, Sn (Sn^{4+} or Sn^{2+}) and V (V^{5+} or V^{4+}) were responsible for the dual electrical property of the VZTO films.

2. EXPERIMENTAL PROCEDURE

2.1. TFT Fabrication. We fabricated inverted-staggered bottom-gate TFTs with three different channel layers (ZTO, VZTO, and VZTO/ZTO) on heavily doped p-type Si substrates with 200-nm-thick thermally grown SiO_2 as a gate insulator. All channel layers were deposited on the substrates at room temperature via radio frequency (RF) magnetron sputtering. First, we used a 4-in. ZTO target with a Zn:Sn atomic ratio of 4:1 for the deposition of the ZTO layer. Second, when depositing the VZTO layer, vanadium was doped by a co-sputtering method using both ZTO and V_2O_3 targets. Last, for the deposition of the VZTO/ZTO bilayer, the VZTO film was co-sputtered *in situ* on the sputtered ZTO film. The channel region was defined by a conventional photolithography and wet etching process. All the defined films were thermally annealed at 350 °C in N_2 gas for 3 h. The Ti/Au/Ti (10/80/10 nm) source and drain (S/D) electrodes were formed by electron beam evaporation at room temperature. Shadow masks were used to define the S/D electrodes, and the channel length (L) and width (W) were 50 and 500 μm, respectively. No passivation layers were deposited. Finally, all the TFTs were thermally annealed at 250 °C in ambient air for 30 min.

2.2. Characterizations of Thin Films. The thickness of the channel layers was checked by a surface profilometer (XP-100, Ambios Technology, Inc.). The V:Zn:Sn composition ratios of the ZTO and VZTO were verified by energy-dispersive spectroscopy (EDS) and were 0:91.6:18.4 and 7.0:77.2:15.8, respectively. Chemical analysis of the films was performed using X-ray photoelectron spectroscopy (XPS) (Theta Probe, Thermo Fisher Scientific Co.).

2.3. TFT Measurements. All the current−voltage ($I−V$) measurements were carried out at room temperature in air using a Model HP-4145B semiconductor parameter analyzer. For light illumination, a 150 W Xe arc lamp (LS-150, ABET Technologies, Inc.) and a monochromator (Monora 200, DONGWOO OPTRON Co., Ltd.) were used. The optical power of the monochromatic light was measured using a UV-enhanced Si detector and was controlled to be 0.1 mW cm^{-2} on the TFT devices.
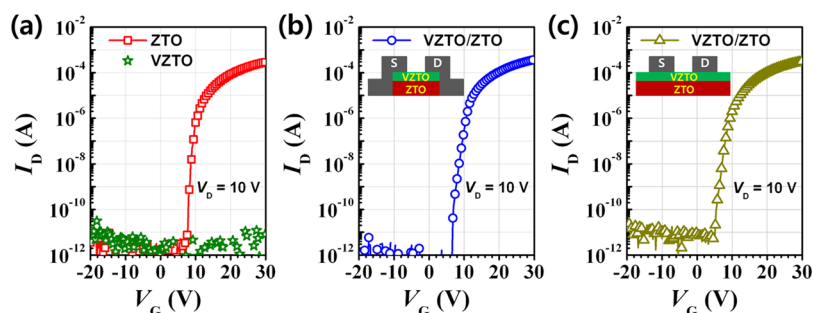
Figure 1. Transfer characteristics of (a) ZTO and VZTO TFTs (b, c) VZTO/ZTO TFTs. The insets in panel (b) or panel (c) show that the S/D electrodes of the VZTO/ZTO TFTs are in contact with both VZTO and ZTO or only with VZTO, respectively.

3. RESULTS AND DISCUSSION

3.1. Anomalous Electrical Behavior of VZTO Thin Films. Figure 1a shows the transfer characteristics of single-layer TFTs using ZTO and VZTO films as channel materials with a thickness of 80 nm each. Here, V_{th} was defined as the gate voltage (V_G), which induces a drain current (I_D) of 1 nA, and the field effect mobility (μ_{FE}) was determined from the transfer data obtained at a low drain voltage ($V_D = 1$ V) by the following equation:

$$\mu_{FE} = \left[\frac{L}{C_i W V_D} \frac{dI_D}{dV_G} \right]_{max} \tag{1}$$

where C_i, W, and L are the gate insulator capacitance per unit area, channel width and length, respectively. The subthreshold swing (SS) value was estimated by

$$SS = \left[\left(\frac{d \log I_D}{dV_G} \right)_{max} \right]^{-1} \tag{2}$$

The single ZTO TFT as a reference exhibited values of $V_{th} = 8.3$ V, $\mu_{FE} = 15.3$ cm^2 V^{-1} s^{-1}, and SS = 0.24 V dec^{-1}. On the other hand, the single VZTO TFT did not have any TFT characteristics. Even at $V_G = 80$ V, no charge carrier accumulation occurred. In this study, we could not measure Hall effect characteristics of the vanadium-doped ZTO thin film, because it had a high electrical resistivity. This indicates that the single VZTO film is a semi-insulator, even though it has an optical band gap of 3.2 eV (see Figure S1 in the Supporting Information). On the other hand, the VZTO/ZTO bilayer TFT shown in Figure 1b exhibited a high electrical performance comparable to that of the single ZTO TFT. Specifically, it showed values of $V_{th} = 7.7$ V, $\mu_{FE} = 16.9$ cm^2 V^{-1} s^{-1}, and SS = 0.44 V dec^{-1}. Here, the electrical transport of the VZTO/ZTO bilayer TFT can be expected to originate from the bottom ZTO layer, because, as shown in the inset of Figure 1b, the S/D electrodes still contact the sides of the bottom ZTO layer, even though the top VZTO layer does not provide an effective conduction path. Thus, in order to confirm whether or not the top VZTO layer in the VZTO/ZTO TFT contributes to charge transport, we fabricated a VZTO/ZTO TFT in which the S/D electrodes only contact the top VZTO layer (40 nm thick). The schematic TFT structure is illustrated in the inset of Figure 1c. This TFT shows the transfer characteristic of a typical TFT. Thus, it is noticeable that the VZTO film in the VZTO/ZTO bilayer has a semiconducting property, unlike the semi-insulating property of the single VZTO film.

In order to investigate the origin of abnormal electrical properties of the VZTO films, which depend on channel structure, XPS measurements were carried out using an Al K$_\alpha$ X-ray source. Before XPS measurements, the surfaces of the films were slightly sputtered by Ar ions to eliminate artifacts from surface contamination. Figure 2 illustrates the XPS spectra
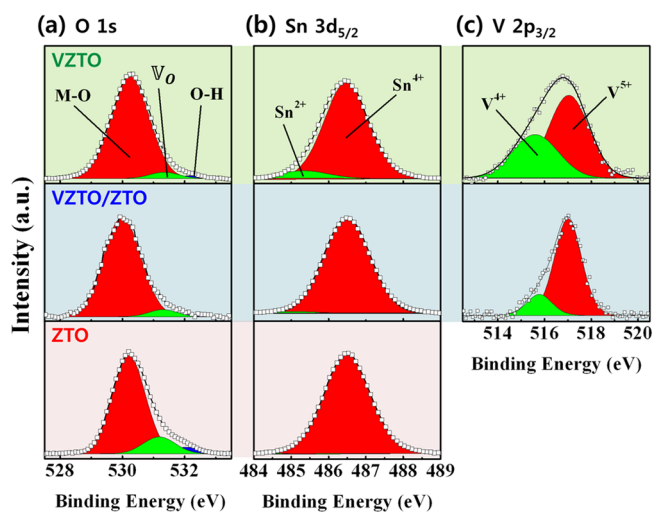
Figure 2. (a) O 1s, (b) Sn 3d$_{5/2}$, and (c) V 2p$_{3/2}$ XPS spectra of ZTO, VZTO/ZTO, and VZTO films.
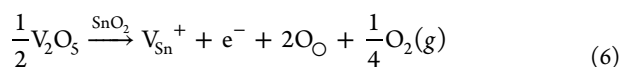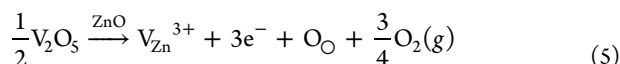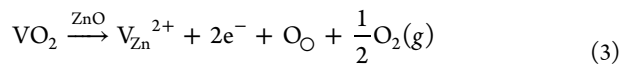
of the O 1s, Sn 3d$_{5/2}$, and V 2p$_{3/2}$ core levels obtained from the ZTO, VZTO, and VZTO on ZTO. The peak centered at 284.5 eV was assigned as the binding energy of the C 1s peak for C−C bonds to calibrate the binding energies of photoelectrons. As shown in Figure 2a, the O 1s spectra were deconvoluted into three peaks centered at binding energies of 530.1 ± 0.1, 531.3 ± 0.1, and 532.1 ± 0.1 eV. The lowest peaks (M−O) at binding energies of 530.1 ± 0.1 eV are attributed to the O^{2-} ions that are fully coordinated with metal cations.[24,25] The medium peaks at 531.3 ± 0.1 eV are from the oxygen vacancies ($\mathbb{V}_O$), and the peaks at 532.1 ± 0.1 eV are from hydroxyl groups (O−H).[24,25] As listed in Table S1 in the Supporting Information), the relative peak area of $\mathbb{V}_O$ in the ZTO film was 13.7% and reduced to 5.3% and 4.5% in VZTO and VZTO/ZTO films, respectively. This result indicates that the V ions act as a $\mathbb{V}_O$ suppressor, as expected. $\mathbb{V}_O$ is well-known as the carrier generator in many oxides, because $\mathbb{V}_O$ can be ionized by thermal energy and can simultaneously eject carrier electrons into the channel layer.[4,27,34] Based on thermodynamics, the carrier concentration originating from $\mathbb{V}_O$ increases with $\mathbb{V}_O$ concen-
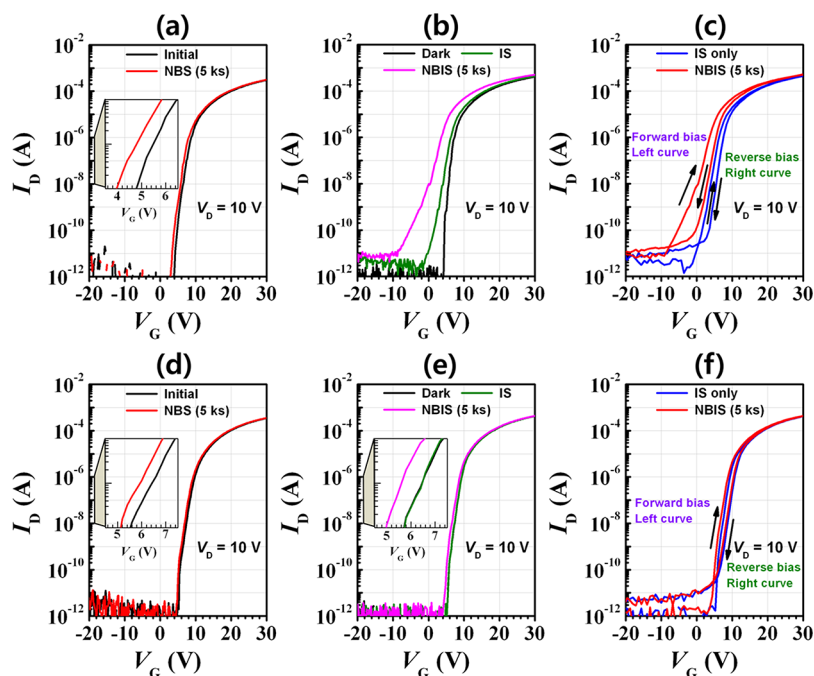
Figure 3. Change in transfer curves of the ZTO TFT under (a) negative-bias stress (NBS) and (b) illumination stress (IS) only and negative bias illumination stress (NBIS). Hysteresis loop of (c) ZTO TFT under IS only or NBIS for 5000 s. As for the VZTO/ZTO bilayer TFT, (d) NBS, (e) IS only and NBIS, and (f) hysteresis. NBS, IS, and NBIS conditions are as follows: (i) NBS: $V_G = -30$ V, duration time = 5000 s; (ii) IS: wavelength = 550 nm), power density = 0.1 mW cm^{-2}, duration time = 5 min; (iii) NBIS: $V_G = -30$ V, wavelength = 550 nm, power density = 0.1 mW cm^{-2}, duration time = 5000 s.

tration ($[\mathbb{V}_O]$). Hence, if $\mathbb{V}_O$ provides the dominant contribution to the total carrier concentration (n_T) of the VZTO films, the carrier concentration of the single VZTO film is similar with or larger than that of the VZTO film in the bilayer when considering the tendency of $[\mathbb{V}_O]$ in the VZTO films. However, this explanation is opposite to our observation. Thus, we took into account the change in the chemical bonding of Sn and V atoms, as shown in Figure 2b and 2c.

Sn and V atoms in oxides appear as multivalent ions. Sn has two ionic forms (Sn^{4+} and Sn^{2+}), and V has four ionic forms (V^{5+}, V^{4+}, V^{3+}, and V^{2+}). The Sn 3d$_{5/2}$ spectra in Figure 2b and Table S2 (Supporting Information) revealed that Sn ions in the semi-insulating VZTO film (single VZTO film) consist of ~10% Sn^{2+} ions and ~90% Sn^{4+} ions. On the other hand, the semiconducting VZTO film in the VZTO/ZTO bilayer shows predominant chemical bonding of Sn^{4+} cations (>98%). In addition, it is very interesting that V 2p$_{3/2}$ spectra between single layers and bilayers are quite different, as shown in Figure 2c. Based on literature sources compiled in the NIST database, V 2p$_{3/2}$ spectra were fitted with two fitting curves, corresponding to V^{4+} and V^{5+}. The semiconducting VZTO film on the ZTO shows the cation distribution of 17% V^{4+} and 83% V^{5+}, while the V cations in the semi-insulating single VZTO film consist of 37% V^{4+} and 63% V^{5+} ions (see Table S3 in the Supporting Information). These results imply that the significant reduction of Sn and V metal ions is strongly related to the semi-insulating behavior of the VZTO film. Recently, we reported that a weak broad shoulder peak located at 33–34° in grazing incidence X-ray diffraction (GIXRD) data of the ZTO films were originated from the amorphous-like phase including locally small crystalline phase.[39] Thus, the concept for the substitution of V ions into Zn or Sn sites can be partly considered as the following reactions:

$$VO_2 \xrightarrow{ZnO} V_{Zn}^{2+} + 2e^- + O_O + \frac{1}{2}O_2(g) \tag{3}$$

$$VO_2 \xrightarrow{SnO_2} V_{Sn}^{\times} + 2O_O \tag{4}$$

$$\frac{1}{2}V_2O_5 \xrightarrow{ZnO} V_{Zn}^{3+} + 3e^- + O_O + \frac{3}{4}O_2(g) \tag{5}$$

$$\frac{1}{2}V_2O_5 \xrightarrow{SnO_2} V_{Sn}^+ + e^- + 2O_O + \frac{1}{4}O_2(g) \tag{6}$$

where V_M is a vanadium atom that occupies a M site (M = Zn, Sn) and is not an oxygen vacancy, which is expressed as $\mathbb{V}_O$. Also, the superscript "×" indicates neutrality. The above reactions (except reaction 4) show that aliovalent V doping in substitutional sites can give carrier electrons, regardless of whether V occurs as V^{4+} or V^{5+}. This may be effective, to some degree, in the semiconducting VZTO on ZTO. For the single VZTO film, the contribution of the ionization of V atoms to n_T is much less than that in the VZTO on ZTO, since the content of V^{5+} ions (which can provide more electrons than V^{4+} ions) decreases from 83% in the VZTO on ZTO to 59% in the single VZTO film. Moreover, much larger reduction of Sn ions from Sn^{4+} to Sn^{2+} is observed in the single VZTO film, given the presence of the shoulder peak coming from Sn^{2+} bonding in Figure 2b. This leads to the generation of holes, which is described as follows:

$$Sn^{4+} \rightarrow Sn^{2+} + 2h^+ \tag{7}$$

Thus, electron charge carriers in the single VZTO film can be compensated by these holes. Meanwhile, there is little reduction of Sn ions from Sn^{4+} to Sn^{2+} in the VZTO on ZTO. Accordingly, the VZTO/ZTO bilayer TFT shows quite good TFT performance, unlike the single VZTO TFT. This
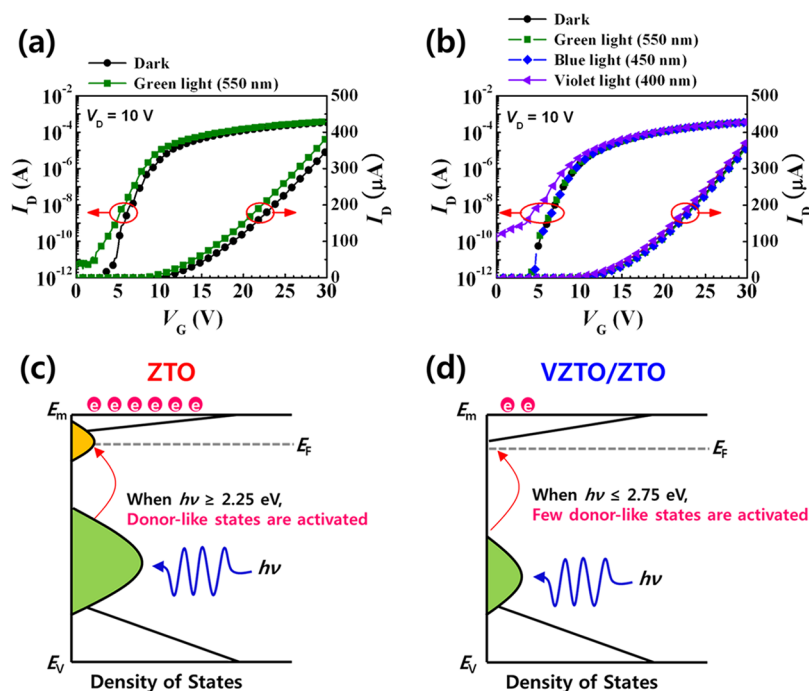
Figure 4. Change in transfer curves of (a) ZTO and (b) VZTO/ZTO TFTs under illumination stress (IS) at various wavelengths (λ = 400, 450, and 550 nm) with a fixed power density (0.1 mW cm^{-2}). Schematic illustrations of the change in the subgap states of (c) ZTO and (d) VZTO/ZTO films under IS.

phenomenon was clearly interpreted with the aid of XPS analysis of Sn and V cation bonding.

3.2. Dramatically Improved Stability of VZTO/ZTO Bilayer TFT. Figures 3a and 3d show the results of negative bias stress (NBS) tests for the ZTO single-layer and VZTO/ZTO bilayer TFTs, respectively, where a V_G value of −30 V was applied for a total duration of 5000 s under dark conditions. The stress was interrupted several times to measure transfer characteristics at a V_D of 10 V. Threshold voltage shift (ΔV_{th}) values of the ZTO and VZTO/ZTO TFTs were estimated to be 1.0 and <0.5 V, respectively, showing better stability of the bilayer TFT than that of the single-layer TFT. The negative ΔV_{th} under NBS is attributed to the screen effect induced by positive charges at the semiconductor/insulator interface or in the near-interface bulk. These positive charges mainly originated from the donor-like states such as neutral oxygen vacancies (V_O), which can capture the minority hole carriers accumulated at/near the interface by NBS and can be positively charged (V_O^{2+}).[8,27] Thus, the reduced ΔV_{th} under NBS in the bilayer TFT indicates decreased donor-like states at the interface and/or near-interface bulk. However, the ΔV_{th} under NBS is relatively trivial.

In order to investigate more practical applicability of the VZTO/ZTO bilayer TFT and the stark difference in stability, the transfer characteristics of ZTO and VZTO/ZTO TFTs were measured under negative-bias illumination stress (NBIS). For the NBIS tests, both an NBS with V_G = −30 V and an illumination stress (IS) with a wavelength of 550 nm (green) and a power density of ~0.1 mW cm^{-2} were simultaneously applied to the two TFT devices. Figures 3b and 3e show the change of transfer characteristics of ZTO and VZTO/ZTO TFTs, respectively, when each device is in darkness, under IS, and NBIS. As shown in Figure 3b, there was a severe change in the transfer characteristics of the ZTO TFT under NBIS. Furthermore, ΔV_{th} values of the ZTO TFT under IS only and

under NBIS for 5000 s were −2.1 V and −7.3 V, respectively. The negative ΔV_{th} under IS can be attributed to the creation of both charged donor-like defects (e.g., V_O^{2+}) and excess carrier electrons by photoexcitation of donor-like defects (e.g., V_O).[7−11,27] Moreover, the SS value of ZTO TFT is severely degraded from 0.24 V dec^{-1} in darkness, to 1.1 V dec^{-1} after IS, and even to 2.6 V dec^{-1} after the NBIS test. The severe degradation of SS values induced by IS indicates that a large amount of the photocreated charged defects are at/near the interface and have an energy level above the flat-band Fermi level (E_{F0}).[9,11] In addition to the creation of ionized donor-like defects by IS, the charged donor-like defects in the bulk can migrate to the interface/near-interface due to the negative bias during NBIS,[8,11] leading to a much larger ΔV_{th} and more severe degradation of SS values than the case of IS or NBS. This degradation mechanism, called the "defect ionization/migration model" here, is supported by the significant change in hysteresis behaviors of ZTO TFTs after IS and NBIS, as shown in Figure 3c. Here, the symbol ΔV_{Hys} is defined as the maximum shift of V_G at the same I_D in the hysteresis loop. The ΔV_{Hys} value is known to be related to the interface trap density and/or near-interface bulk trap density above E_{F0}.[18,40] Furthermore, the ΔV_{Hys} value of the ZTO TFT significantly increased from 2.0 V under IS to 5.1 V after NBIS for 5000 s. This photobias-induced hysteresis creation indicates that a significant increase in the interface trap density and/or near-interface bulk trap density in the ZTO TFT occurred due to NBIS.[40] Unlike the poor stability of the ZTO TFT under IS and NBIS, the VZTO/ZTO bilayer TFT showed a dramatically improved stability under both IS and NBIS. As shown in Figure 3e, the transfer characteristics of the VZTO/ZTO bilayer TFT under IS changed only slightly, compared to that in darkness. Even after NBIS for 5000 s, there was a very small ΔV_{th} value of 0.9 V and SS values were almost unchanged, as is apparent in Figure 3f. In addition, the ΔV_{Hys} values of the VZTO/ZTO TFT were

almost unchanged after NBIS for 5000 s (~0.3 V). This indicates that the VZTO/ZTO has few donor-like defects, which can be activated by a photon energy of 550-nm wavelength (2.25 eV) to affect the transfer characteristics of the TFT.

To obtain more insight into the defect level in the bandgap, we performed IS tests with an illumination source of various wavelengths, as shown in Figures 4a and 4b. The severe SS degradation of the single ZTO TFT starts with green light energy of 550 nm (2.25 eV). On the other hand, the VZTO/ZTO bilayer TFT is almost unchanged under illumination stress, even with a blue wavelength of 450 nm (2.75 eV), and exhibits SS degradation by the irradiation of near UV photon energy (~400 nm), which is near the optical bandgap of the single ZTO film (3.0 eV; see Figure S1 in the Supporting Information). This indicates that the VZTO/ZTO bilayer has few donor-like states that can be activated and donate charge carriers by photons with energies of ≤2.75 eV, as illustrated in Figure 4d. In contrast, the single ZTO film has a great deal of the subgap states that can be activated by low-energy irradiation (Figure 4c).

4. CONCLUSION

We have suggested a novel channel design to incorporate multivalent metal cations for the fabrication of oxide thin-film transistors (TFTs) with both high electrical performance and high stability. The addition of multivalent V atoms into indium-free ZTO films induced a dual electrical performance, depending on the channel structure. The VZTO/ZTO channel structure exhibited relatively good TFT performance without degradation of mobility, while the VZTO TFT had no typical TFT transfer characteristics. XPS analyses revealed that the semi-insulating behavior of the single VZTO film was attributed to the existence of more V^{4+} and a significant reduction of Sn^{4+} to Sn^{2+} ions. In NBIS tests, it was found that the VZTO/ZTO TFT had much better stability than the single ZTO TFT. Under IS tests of various wavelengths, dramatically improved stability of the VZTO/ZTO TFT was observed due to the reduction of donor-like states that can be positively ionized by blue and green illumination. Therefore, doping with a multivalent elemental vanadium in the ZTO film and the use of a VZTO/ZTO channel structure are expected to provide a feasible strategy for highly reliable performance of the oxide-based TFT devices.

■ ASSOCIATED CONTENT

Ⓢ Supporting Information

O 1s XPS results for ZTO, VZTO/ZTO, and VZTO films; Sn $3d_{5/2}$ XPS results for ZTO, VZTO/ZTO, and VZTO films; V $2p_{3/2}$ XPS results for VZTO/ZTO and VZTO films; transmittance of the ZTO and VZTO films on glass substrates. This material is available free of charge via the Internet at http://pubs.acs.org.

■ AUTHOR INFORMATION

Corresponding Author

* E-mail: chohk@skku.edu.

Notes

The authors declare no competing financial interest.

■ ABBREVIATIONS

AOS = amorphous oxide semiconductor
AMLCD = active matrix liquid crystal display
AMOLED = active matrix organic light-emitting diode
ZTO = zinc tin oxide
VZTO = vanadium-doped zinc tin oxide
XPS = X-ray photoelectron spectroscopy
NBS = negative-bias stress
IS = illumination stress
NBIS = negative-bias illumination stress

■ REFERENCES

(1) Chiang, H. Q.; Wager, J. F.; Hoffman, R. L.; Jeong, J.; Keszler, D. A. High Mobility Transparent Thin-Film Transistors with Amorphous Zinc Tin Oxide Channel Layer. *Appl. Phys. Lett.* **2005**, *86*, 013503-1−013503-3.

(2) Dehuff, N. L.; Kettenring, E. S.; Hong, D.; Chiang, H. Q.; Wager, J. F.; Hoffman, R. L.; Park, C. H.; Keszler, D. A. Transparent Thin-Film Transistors with Zinc Indium Oxide Channel Layer. *J. Appl. Phys.* **2005**, *97*, 064505-1−064505-5.

(3) Chiang, H. Q.; Hong, D.; Hung, C. M.; Presley, R. E.; Wager, J. F.; Park, C. H.; Keszler, D. A.; Herman, G. S. Thin-Film Transistors with Amorphous Indium Gallium Oxide Channel Layers. *J. Vac. Sci. Technol., B* **2006**, *24*, 2702−2705.

(4) Nomura, K.; Ohta, H.; Takagi, A.; Kamiya, T.; Hirano, M.; Hosono, H. Room-Temperature Fabrication of Transparent Flexible Thin-Film Transistors Using Amorphous Oxide Semiconductors. *Nature* **2004**, *432*, 488−492.

(5) Park, J. S.; Kim, T. S.; Son, K. S.; Lee, K. H.; Maeng, W. J.; Kim, H. S.; Kim, E. S.; Park, K. B.; Seon, J. B.; Choi, W.; Ryu, M. K.; Lee, S. Y. The Influence of SiO_x and SiN_x Passivation on the Negative Bias Stability of Hf−In−Zn−O Thin Film Transistors under Illumination. *Appl. Phys. Lett.* **2010**, *96*, 262109-1−262109-3.

(6) Park, J. S.; Kim, T. S.; Son, K. S.; Jung, J. S.; Lee, K. H.; Kwon, J. Y.; Koo, B.; Lee, S. Influence of Illumination on the Negative-Bias Stability of Transparent Hafnium−Indium−Zinc Oxide Thin-Film Transistors. *IEEE Electron Device Lett.* **2010**, *31*, 440−442.

(7) Kwon, J. Y.; Jung, J. S.; Son, K. S.; Lee, K. H.; Park, J. S.; Kim, T. S.; Park, J. S.; Choi, R.; Jeong, J. K.; Koo, B.; Lee, S. Y. The Impact of Gate Dielectric Materials on the Light-Induced Bias Instability in Hf−In−Zn−O Thin Film Transistor. *Appl. Phys. Lett.* **2010**, *97*, 183503-1−183503-3.

(8) Oh, H.; Yoon, S. M.; Ryu, M. K.; Hwang, C. S.; Yang, S.; Park, S. H. K. Transition of Dominant Instability Mechanism Depending on Negative Gate Bias under Illumination in Amorphous In−Ga−Zn−O Thin Film Transistor. *Appl. Phys. Lett.* **2011**, *98*, 033504−1−033504−3.

(9) Huang, X. M.; Wu, C. F.; Lu, H.; Ren, F. F.; Xu, Q. Y.; Ou, H. L.; Zhang, R.; Zheng, Y. D. Electrical Instability of Amorphous Indium−Gallium−Zinc Oxide Thin Film Transistors under Monochromatic Light Illumination. *Appl. Phys. Lett.* **2012**, *100*, 243505−1−243505−4.

(10) Migliorato, P.; Chowdhury, M. D. H.; Um, J. G.; Seok, M.; Jang, J. Light/Negative Bias Stress Instabilities in Indium Gallium Zinc Oxide Thin Film Transistors Explained by Creation of a Double Donor. *Appl. Phys. Lett.* **2012**, *101*, 123502-1−123502-5.

(11) Um, J. G.; Mativenga, M.; Migliorato, P.; Jang, J. Increase of Interface and Bulk Density of States in Amorphous-Indium−Gallium−Zinc−Oxide Thin-Film Transistors with Negative-Bias-under-Illumination-Stress Time. *Appl. Phys. Lett.* **2012**, *101*, 113504−1−113504−4.

(12) Chen, T. C.; Chang, T. C.; Hsieh, T. Y.; Tsai, C. T.; Chen, S. C.; Lin, C. S.; Hung, M. C.; Tu, C. H.; Chang, J. J.; Chen, P. L. Light-

Induced Instability of an InGaZnO Thin Film Transistor with and without SiO$_x$ Passivation Layer Formed by Plasma-Enhanced-Chemical-Vapor-Deposition. *Appl. Phys. Lett.* **2010**, *97*, 192103-1−192103-3.

(13) Yang, S.; Cho, D. H.; Ryu, M. K.; Park, S. H. K.; Hwang, C. S.; Jang, J.; Jeong, J. K. Improvement in the Photon-Induced Bias Stability of Al−Sn−Zn−In−O Thin Film Transistors by Adopting AlO$_x$ Passivation Layer. *Appl. Phys. Lett.* **2010**, *96*, 213511-1−213511-3.

(14) Moon, Y. K.; Lee, S.; Kim, W. S.; Kang, B. W.; Jeong, C. O.; Lee, D. H.; Park, J. W. Improvement in the Bias Stability of Amorphous Indium Gallium Zinc Oxide Thin-Film Transistors Using an O$_2$ Plasma-Treated Insulator. *Appl. Phys. Lett.* **2009**, *95*, 013507−1−013507−3.

(15) Yang, S.; Ji, K. H.; Kim, U. K.; Hwang, C. S.; Park, S. H. K.; Hwang, C. S.; Jang, J.; Jeong, J. K. Suppression in the Negative Bias Illumination Instability of Zn−Sn−O Transistor Using Oxygen Plasma Treatment. *Appl. Phys. Lett.* **2011**, *99*, 102103−1−102103−3.

(16) Yang, B. S.; Park, S.; Oh, S.; Kim, Y. J.; Jeong, J. K.; Hwang, C. S.; Kim, H. J. Improvement of the Photo-Bias Stability of the Zn−Sn−O Field Effect Transistors by an Ozone Treatment. *J. Mater. Chem.* **2012**, *22*, 10994−10998.

(17) Oh, H.; Park, S. H. K.; Hwang, C. S.; Yang, S.; Ryu, M. K. Enhanced Bias Illumination Stability of Oxide Thin Film Transistor through Insertion of Ultrathin Positive Charge Barrier into Active Material. *Appl. Phys. Lett.* **2011**, *99*, 022105-1−022105-3.

(18) Yun, M. G.; Kim, S. H.; Ahn, C. H.; Cho, S.; Cho, H. K. Effects of Channel Thickness on Electrical Properties and Stability of Zinc Tin Oxide Thin-Film Transistors. *J. Phys. D: Appl. Phys.* **2013**, *46*, 475106.

(19) Park, J. C.; Kim, S.; Kim, S.; Kim, C.; Song, I.; Park, Y.; Jung, U. I.; Kim, D. H.; Lee, J. S. Highly Stable Transparent Amorphous Oxide Semiconductor Thin-Film Transistors Having Double-Stacked Active Layers. *Adv. Mater.* **2010**, *22*, 5512−5516.

(20) Kim, H. S.; Park, J. S.; Jeong, H. K.; Son, K. S.; Kim, T. S.; Seon, J. B.; Lee, E.; Chung, J. G.; Kim, D. H.; Ryu, M.; Lee, S. Y. Density of States-Based Design of Metal Oxide Thin-Film Transistors for High Mobility and Superior Photostability. *ACS Appl. Mater. Interfaces* **2012**, *4*, 5416−5421.

(21) Ahn, C. H.; Senthil, K.; Cho, H. K.; Lee, S. Y. Artificial Semiconductor/Insulator Superlattice Channel Structure for High-Performance Oxide Thin-Film Transistors. *Sci. Rep.* **2013**, *3*, 2737.

(22) Jung, H. Y.; Kang, Y.; Hwang, A. Y.; Lee, C. K.; Han, S.; Kim, D. H.; Bae, J. U.; Shin, W. S.; Jeong, J. K. Origin of the Improved Mobility and Photo-Bias Stability in a Double-Channel Metal Oxide Transistor. *Sci. Rep.* **2014**, *4*, 3765.

(23) Choi, H. S.; Jeon, S.; Kim, H.; Shin, J.; Kim, C.; Chung, U. I. Influence of Hf Contents on Interface State Properties in α-HfInZnO Thin-Film Transistors with SiN$_x$/SiO$_x$ Gate Dielectrics. *Appl. Phys. Lett.* **2011**, *99*, 183502-1−183502-3.

(24) Seo, S. J.; Jeon, J. H.; Hwang, Y. H.; Bae, B. S. Improved Negative Bias Illumination Instability of Sol−Gel Gallium Zinc Tin Oxide Thin Film Transistors. *Appl. Phys. Lett.* **2011**, *99*, 152102-1−152102-3.

(25) Yang, B. S.; Huh, M. S.; Oh, S.; Lee, U. S.; Kim, Y. J.; Oh, M. S.; Jeong, J. K.; Hwang, C. S.; Kim, H. J. Role of ZrO$_2$ Incorporation in the Suppression of Negative Bias Illumination-Induced Instability in Zn−Sn−O Thin Film Transistors. *Appl. Phys. Lett.* **2011**, *98*, 122110-1−122110-3.

(26) Kim, J. H.; Kim, U. K.; Chung, Y. J.; Hwang, C. S. Correlation of the Change in Transfer Characteristics with the Interfacial Trap Densities of Amorphous In−Ga−Zn−O Thin Film Transistors under Light Illumination. *Appl. Phys. Lett.* **2011**, *98*, 232102-1−232102-3.

(27) Noh, H. K.; Chang, K. J.; Ryu, B.; Lee, W. J. Electronic Structure of Oxygen-Vacancy Defects in Amorphous In−Ga−Zn−O Semiconductors. *Phys. Rev. B* **2011**, *84*, 115205-1−115205-8.

(28) Oh, S.; Yang, B. S.; Kim, Y. J.; Oh, M. S.; Jang, M.; Yang, H.; Jeong, J. K.; Hwang, C. S.; Kim, H. J. Anomalous Behavior of Negative Bias Illumination Stress Instability in an Indium Zinc Oxide Transistor: A Cation Combinatorial Approach. *Appl. Phys. Lett.* **2012**, *101*, 092107-1−092107-5.

(29) Kamiya, T.; Nomura, K.; Hosono, H. Origins of High Mobility and Low Operation Voltage of Amorphous Oxide TFTs: Electronic Structure, Electron Transport, Defects and Doping. *J. Disp. Technol.* **2009**, *5*, 468−483.

(30) Tanaka, I.; Oba, F.; Tatsumi, K.; Kunisu, M.; Nakano, M.; Adachi, H. Theoretical Formation Energy of Oxygen-Vacancies in Oxides. *Mater. Trans.* **2002**, *43*, 1426−1429.

(31) Mellan, T. A.; Grau-Crespo, R. Density Functional Theory Study of Rutile VO$_2$ Surfaces. *J. Chem. Phys.* **2012**, *137*, 154706-1−154706-8.

(32) Luo, Y. R. *Comprehensive Handbook of Chemical Bond Energies*; CRC Press: Boca Raton, FL, 2007.

(33) Lange, N. A.; Speight, J. G. *Lange's Handbook of Chemistry*, 16th Edition; McGraw−Hill: New York, 2005.

(34) Nomura, K.; Takagi, A.; Kamiya, T.; Ohta, H.; Hirano, M.; Hosono, H. Amorphous Oxide Semiconductors for High-Performance Flexible Thin-Film Transistors. *Jpn. J. Appl. Phys.* **2006**, *45*, 4303−4308.

(35) Janotti, A.; Van de Walle, C. G. Hydrogen Multicentre Bonds. *Nat. Mater.* **2007**, *6*, 44−47.

(36) Kamiya, T.; Nomura, K.; Hirano, M.; Hosono, H. Electronic Structure of Oxygen Deficient Amorphous Oxide Semiconductor α-InGaZnO$_{4-x}$: Optical Analyses and First-Principle Calculations. *Phys. Status Solidi C* **2008**, *5*, 3098−3100.

(37) Oba, F.; Choi, M.; Togo, A.; Tanaka, I. Point Defects in ZnO: An Approach from First Principles. *Sci. Technol. Adv. Mater.* **2011**, *12*, 034302.

(38) Kim, H. S.; Park, J. S.; Maeng, W. J.; Son, K. S.; Kim, T. S.; Ryu, M.; Lee, J.; Lee, J. C.; Ko, G.; Im, S.; Lee, S. Y. The Influence of In/Zn Ratio on the Performance and Negative-Bias Instability of Hf−In−Zn−O Thin-Film Transistors under Illumination. *IEEE Electron Device Lett.* **2011**, *32*, 1251−1253.

(39) Kim, S. H.; Ahn, C. H.; Yun, M. G.; Cho, S. W.; Cho, H. K. Anomalous Tin Chemical Bonding in Indium−Zinc−Tin Oxide Films and Their Thin Film Transistor Performance. *J. Phys. D: Appl. Phys.* **2014**, *47*, 485101.

(40) Jo, J. W.; Kim, Y. H.; Park, S. K. Light-Induced Hysteresis and Recovery Behaviors in Photochemically Activated Solution-Processed Metal-Oxide Thin-Film Transistors. *Appl. Phys. Lett.* **2014**, *105*, 043503-1−043503-5.